J. Fluid Mech. (1993), *vol.* 247, *pp.* 137–156

Boundary interactions for two-dimensional granular flows. Part 2. Roughened boundaries

By CHARLES S. CAMPBELL

Department of Mechanical Engineering, University of Southern California, Los Angeles, CA 90089–1453 USA

(Received 24 January 1992 and in revised form 6 August 1992)

The global behaviour of a granular flow is critically dependent on its interaction with whatever solid boundaries with which it comes into contact, whether they be used to drive, retard or simply bound the flow field. This paper describes the results of a computer simulation study of the effects of roughening boundaries by 'gluing' particles to the surfaces. Roughness is commonly used in experimental devices as a way of approximating a no-slip condition between a granular material and the driving surfaces. On a microscopic level, this produces a boundary that extends out into the flow field to the limit of the roughness elements. This has a strong effect on the way that forces, and, in particular, torque, is transmitted to the particles in the neighbourhood of the boundary.

1. Introduction

When studying granular flows, it is common to roughen solid boundaries of experimental devices to try and impose the equivalent of a no-slip condition. Typically, this is accomplished by gluing onto the surface particles of roughly the same size as the test material. This is done in the belief that the glued particles will be indistinguishable from the free particles in the immediate neighbourhood of the boundary and will force their free brothers to follow their motion. Such a belief is somewhat naive for two reasons. The first is that the glued particle size and spacing affects the ability of the free particles to penetrate into and interact with the layer of glued particles – strongly altering the effective mechanical contact between the boundary and the flowing material. The second difference, one that will be shown to be critical, is that, unlike their free counterparts, the glued particles are not free to rotate. This latter is particularly important in the light of the results for various flat wall boundary conditions, published in Part 1, Campbell (1993), which indicate that the entire behaviour of the flow is critically dependent on the way that the boundary transmits torque to the flow particles.

The idea of a roughened wall has interesting implications from a continuum mechanical viewpoint. In most boundary value problems, the boundary is assumed to be a flat surface and it seems reasonable to expect that, as long as the dimensions of the system are large compared to the size of roughness elements, such an approximation is valid for rough walls. However, a flat boundary can only specify the components of the stress tensor in the directions normal and tangential to the boundary surface; all the other components are generated internally to the flowing material as reactions to the applied stresses. Part 1 of this study shows that this results in locally asymmetric stress tensors whose asymmetry is balanced by the generation of locally non-zero couple stresses. However, if the boundary is roughened,

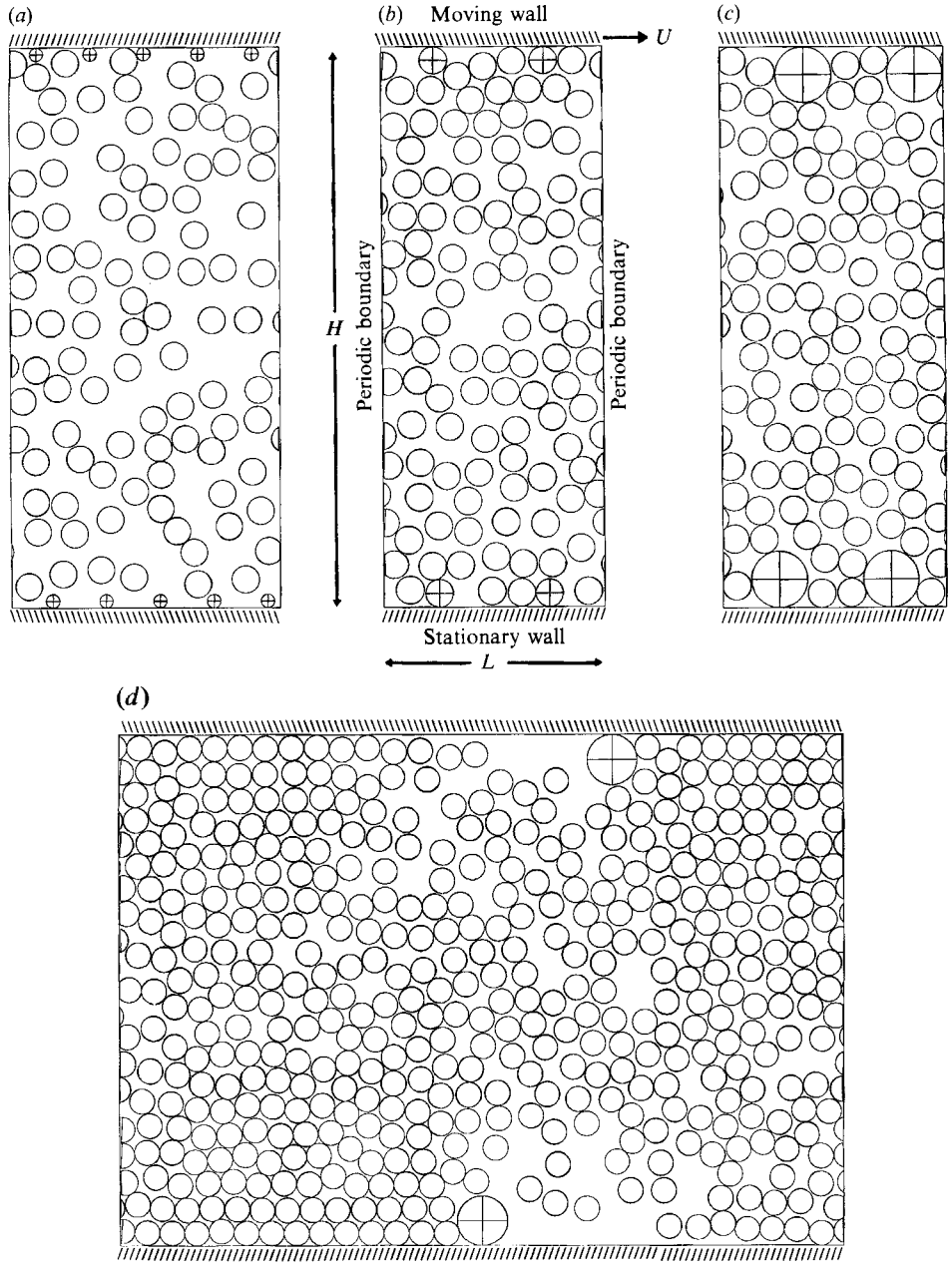

FIGURE 1. Four snapshots of the computer simulation control volume. The glued particles are marked with crosses. (*a*) $\bar{\nu} = 0.45$, $R_G/R = 0.5$, $S_G/R_G = 8$; (*b*) $\bar{\nu} = 0.65$, $R_G/R = 1$, $S_G/R_G = 8$; (*c*) $\bar{\nu} = 0.65$, $R_G/R = 2$, $S_G/R_G = 4$; (*d*) $\bar{\nu} = 0.65$, $R_G/R = 2$, $S_G/R_G = 32$.

it penetrates into the flowing material and thus, in a sense, specifies, or at least affects, *all* of the components of the stress tensor. On a microscopic level, this is easily understood as the stresses are ultimately the result of particle collisions, and glued–free particle collisions make much the same contribution to all the components of the stress tensor as do free–free particle collisions (while a collision between a free

particle and a flat wall will only exert forces in the directions normal and tangential to the surfaces). It is not immediately clear how such an effect can be interpreted in a continuum mechanical sense, but it is apparent that a rough boundary may have a strong effect on the symmetry of the stress tensor and the consequent couple stress generation.

Roughened boundaries are also a favourite model for analytical studies based on kinetic theory ideas. There has not yet been a successful kinetic theory model that includes appreciable degrees of particle surface friction and thus there is no obvious mechanism by which a flat boundary might apply a shear force to the flowing material. But, as they extend outward into the flowing material, bumpy boundaries can apply a shear force to a frictionless material through the geometry of the collisions between the roughness elements and the flowing material. Jenkins & Richman (1986) developed a set of boundary conditions for two-dimensional smooth circular-disc flows in the neighbourhood of a boundary composed of semicircular bumps glued to a flat wall. This work was later extended by Richman & Chou (1988), Richman (1988) and Hanes, Jenkins & Richman (1988). Louge, Jenkins & Hopkins (1990) have performed a computer simulation study that confirms the Hanes *et al.* results. Richman & Marciniec (1990) analysed the flow down an inclined chute with a bumpy bottom boundary. These analyses are particularly appealing as they extrapolate from fundamental properties of the free and glued particles to the behaviour of the entire flow field. Different rough boundary characteristics have also been used to explain the vastly different results obtained from shear cell studies by Savage & Sayed (1984), Hanes & Inman (1985) and Craig, Buckholtz & Domato (1987).

This paper studies the problem of how frictional particles interact with rough, frictional walls. This is somewhat more complicated than the smooth particle case as the interactions between glued and free particles, and between free particles and the walls, apply torques to the particles. A preliminary report of this work may be found in Campbell & Gong (1987).

2. Computer simulation

The results of this study are derived from a computer simulation of a Couette flow of two-dimensional disks. The major difference between this simulation and that used in Part 1, Campbell (1993) is the nature of the solid walls that bound the top and bottom of the control volume and drive the flow. In this paper, for the flat portions of the wall, like the Type A boundaries studied in Part 1, it is assumed that, on departure after a collision with the wall, there is no relative velocity between the particle surface and the wall. In addition, the walls are roughened by 'gluing' particles of radius R_G whose centres are spaced a distance S_G apart. This is illustrated in the snapshots in figure 1. Glued particles follow the velocity of the wall exactly and are prevented from rotating, but, in all other ways are identical to the free particles in their flow, i.e. those particles possess the same coefficient of restitution and surface frictional properties. However, as the velocity of a glued particle cannot change, it is treated in the collision solution as if its mass was infinite relative to that of a free particle.

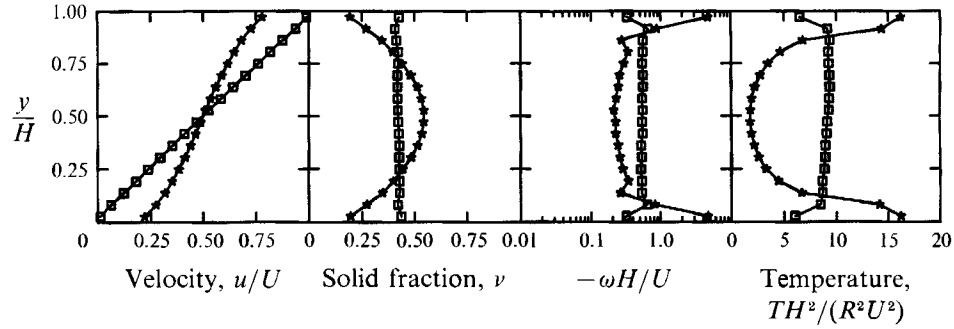

FIGURE 2. A comparison of the results from smooth walls (★) and rough walls (□) ($R_G/R = 1$, $S_G/R_G = 8$) at a mean solid concentration, $\bar{\nu} = 0.45$.

3. General features of the flow field

As a point of reference, figure 2 shows a comparison between the results obtained from smooth and rough boundaries. Shown are: the velocity u scaled by the top wall velocity U, the solid fraction ν (a dimensionless density equal to the fraction of a unit volume occupied by solid particles), the rotational velocity ω, scaled by the apparent shear rate U/H, and the granular temperature T, also scaled by the apparent velocity gradient (T has units of (velocity)^2, so that it appears in the dimensionless form TH^2/R^2U^2.) All are plotted as functions of the vertical coordinate, y, divided by the separation, H, of the solid boundaries. The two sets of data are the results of a smooth wall (Type A) simulation (the closed star-like symbols) and of a rough wall defined by $R_G/R = 1$ (i.e. the glued particles have the same radius as the free particles) and a spacing, $S_G/R_G = 8$. Both simulations were run for a mean solid fraction $\bar{\nu} = 0.45$ and a wall separation $H/R = 40$.

The two results are surprisingly different. The smooth wall results show a large slip velocity and elevated velocity gradients in the neighbourhood of the wall. These zones of large shear correspond to regions of reduced solid fraction and elevated granular temperature. (As the pressure is roughly uniform across the control volume, this is an illustration that, globally, these systems obey some sort of equation of state relating the pressure, density and granular temperature.) As one would expect, the rotational velocity is large in the neighbourhood of the wall, as the particles will nearly roll in reaction to the slip velocity. This yields an angular velocity profile with a jagged shape as a result of a competition between two modes of generating rotation which are discussed in detail in Part 1 (see figure 4 in that paper). However, roughening the walls produces vastly different results. This time, there is no slip on the wall and the velocity gradient is uniform across the channel. Furthermore, the solid fraction, rotational velocity and granular temperature distributions are nearly uniform outside the points plotted nearest the walls, which are, of course, strongly influenced by the glued particles. (Note, the presence of the glued particles is only reflected in the solid fraction profiles; only the free particles are sampled for the other distributions.)

Now, the large temperature gradients leading away from the wall indicate that the smooth (Type A) boundary acts as a large source of granular temperature. The temperature generated at the boundary is then conducted away from the walls, along the temperature gradients, towards the centre of the flow. No such gradients exist for the roughened boundary, indicating that this boundary is relatively neutral with respect to temperature generation or dissipation. Note, that, directly next to the

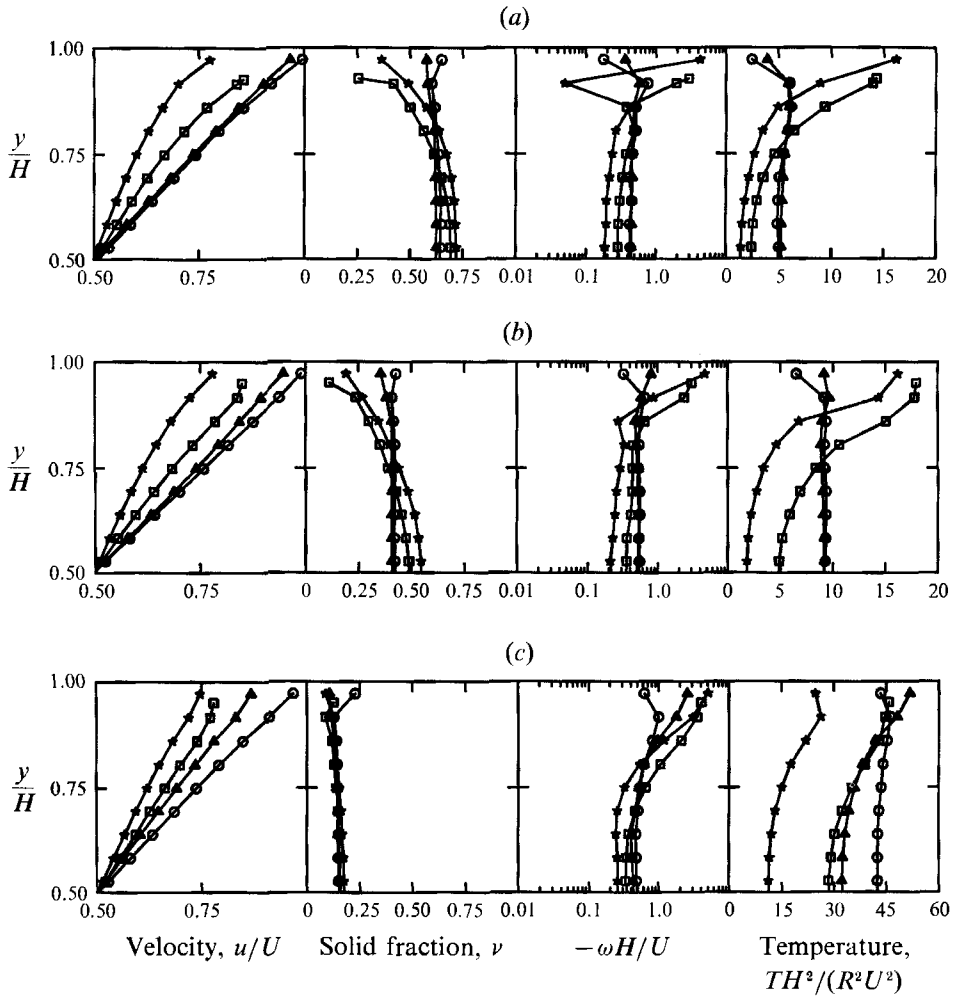

FIGURE 3. The effect of varying the glued particle spacing for three values of the solid concentration: (*a*) $\bar{\nu} = 0.65$, (*b*) $\bar{\nu} = 0.45$ and (*c*) $\bar{\nu} = 0.15$. For all of the roughness elements, $R_G/R = 1$. □, $S_G/R_G = 2$; ○, $S_G/R_G = 8$; △, $S_G/R_G = 32$; ★, smooth. In order to show the boundary region more clearly, only the top half of the control volume is plotted.

walls, where the free particles become trapped between the glued particles, the roughened boundary shows a slight deficit of granular temperature. (This is very similar to the Type B boundaries described in Part 1.) But, as the effect is confined to the glued particle layer, and does not extend further outward into the flow, it is probably not appropriate to consider this type of boundary as a temperature sink – at least not on continuum scales. All of the theoretical studies for frictionless particles, referred to in the introduction, have realized the importance of the production/generation of granular temperature at boundaries.

Part 1 indicated that the global flow is strongly influenced by the way that torque is applied by the boundaries and it is possible to interpret the difference between the smooth and rough wall results solely in those terms. In particular, the large local rotation rate induced by the slip velocity between a smooth boundary and a particle was shown to be converted into granular temperature, making the wall a source of granular temperature. On a macroscopic level, one might say that the rough case

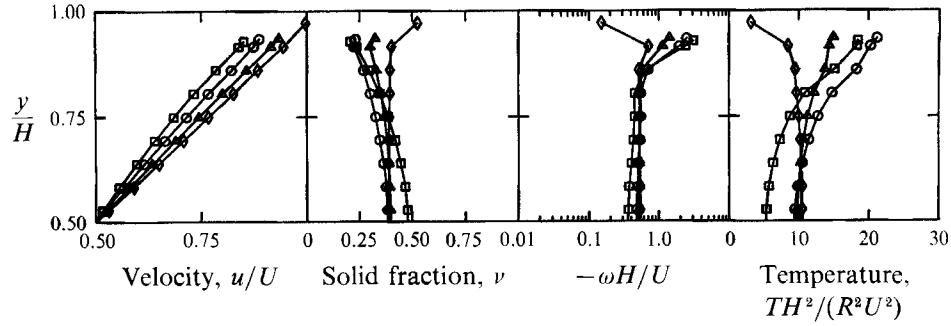

FIGURE 4. The transition from the 'smooth' character of the close-packed ($R_G/R = 1$, $S_G = 2$) to rough wall behaviour by small increase in the particle spacing to $R_G/R = 1$, $S_G = 4.1$. For all cases, $\bar{\nu} = 0.45$. □, $S_G/R_G = 2$; ○, 2.5; △, 3; ◇, 4.1.

generates little rotation simply because there is little slip velocity and, consequently, no velocity difference between the particles and the wall to induce rotation. However, the rotational velocity distribution shows that the roughness actually depresses the rotation rate at the wall. That mechanism may be understood by realizing that, as the roughening particles cannot rotate, they will apply countertorques to any rotating particles that collide with them, leading to a locally reduced average rotation rates. This would be the case as long as the relative translational velocity between the free and roughening particles is small – as it is within the layer of roughened particles near the wall. If the opposite is true, such as in a collision on the outermost edge of a roughening particle, there may be significant rotation generated, just as in a collision with a smooth wall; this last mechanism is apparent in a slightly elevated rotation rate in the second point out from either wall.

Figure 3 shows the effects of varying the spacing of glued particles for three different values of the mean solid fraction ($\bar{\nu} = 0.65$, 0.45 and 0.15). In each case, results are plotted for $R_G/R = 1$ and $S_G/R_G = 2$, 8 and 32, and to show the boundary region more clearly, only the top half of the control volume is plotted. Note that for $S_G/R_G = 2$, the glued particles are tightly packed along the wall and free particles cannot penetrate far into the layer; consequently, the vertical position of the points nearest the wall is altered to reflect the degree of free-particle penetration. Also plotted, for comparison, is the corresponding smooth wall distribution. There are two interesting things to observe in these figures. The first is that the glued particle packing, which contains the largest concentration of glued particles on the wall, $S_G/R_G = 2$, shows most of the characteristics of the flat wall. In such a case, the free particles see only the gentle undulations of the outer surfaces of the glued particles, and, consequently, see a nearly smooth surface. Spacing the glued particles further apart allows greater penetration of free particles into the glued layer and, consequently, reveals an effectively rougher wall. This process occurs fairly quickly; figure 4 shows that the transition from the 'smooth' behaviour of $S_G = 2R_G$, to a fully rough condition has occurred by a spacing of $S_G = 4.1R_G$, which is nearly† the smallest spacing that permits the free particles access to the flat wall. With a further

† Technically, $S_G/R_G = 4$ is the smallest glued particle spacing for which $R = R_G$ free particles have access to the wall. However, in that case, the free particles that manage to penetrate to the wall tend to remain there, held in place by the frictional interaction with their glued neighbours. The net effect is to present a nearly smooth wall to the remaining free particles that mimics the $S_G/R_G = 2$ case. $S_G/R_G = 4.1$ was used to space the particles slightly further apart so that the free particle cannot interact simultaneously with both of its glued neighbours and cannot be held so tightly in place.

increase in the free particle spacing, the completely smooth wall state must be asymptotically approached. Returning to figure 3, it can be seen that, by $S_G/R_G = 8$, free particles may penetrate to the flat wall as there is an open wall area of two particle diameters between the glued particles. This is the case plotted in figure 2 and appears to be the 'roughest' boundary choice used in this study. Surprisingly, for higher $\bar{\nu}$, similar behaviour is seen even for $S_G/R_G = 32$ (with an open area of 15 particle diameters between glued particles), from which one would have expected nearly smooth wall behaviour. But notice that the situation does not extend to the low-density cases. This behaviour may be understood by referring to figure 1(*d*). There, one can see that free particles extend along the wall for over twenty particle diameters in front of a glued particle, effectively increasing its range of influence in the sense that a collision with any of the free particles along the wall will be quickly transmitted along the layer to the nearest glued particle. However, if the average solid concentration is small, it is unlikely that many free particles would gather in the gap, and the glued particles will lose their extended range of influence. Thus, in a sense, $S_G/R_G = 32$ acts like a rough boundary for large free-particle concentrations, but like a smooth boundary at dilute concentrations. Further evidence for this may be found in the granular temperature profiles, which, with significant gradients of temperature pointing towards the $S_G/R_G = 32$ boundary at small $\bar{\nu}$, acts like a source of granular temperature, but is neutral with respect to temperature generation/dissipation at larger $\bar{\nu}$. This is a clear demonstration that the characteristics of a boundary cannot be separated from the characteristics of the flowing material that it bounds.

Figure 5 shows the effect of varying the size of the roughening particles in the three ranges, $R_G/R = 0.5$, 1.0 and 2.0, for the same three concentrations used for figure 3. All of these cases used a glued particle spacing of $S_G/R_G = 8$, which figure 3 indicates as an extremely 'rough' boundary type. The results are pretty much as would be expected. There is noticeably more slip for the $R_G/R = 0.5$ data than for the $R_G/R = 1.0$ data. For the $R_G/R = 2.0$ data, there is almost no velocity gradient for the two points nearest the wall, as these are sampled from within the glued particle layer; this indicates that the free particle nearest the boundary are strongly held between, and pulled along with, the roughening particles. Furthermore, the particles nearest the wall in the $R_G/R = 2.0$ case show almost no rotation and a substantially reduced granular temperature. But one cannot really say that increasing the size of the roughening particles increases the 'roughness' of the surface. In the $R_G/R = 2.0$ case, should the particles nearest the wall be taken as part of the flow or as part of the boundary with which the flowing particles interact? After all, like their glued counterparts, the free particles near the boundary show (i) the same velocity as the wall, (ii) little granular temperature and (iii) significantly reduced rotation rate and therefore behave nearly as if they themselves are glued. It is, perhaps, best to consider that the first two layers of free particles have been drafted into the service of the larger glued particles and have effectively joined the boundary. From a continuum point of view, it may be best to assume that the flow field begins further away from the wall, near the outer edge of the glued particles. Note also that there are strong granular temperature gradients near the wall of the $R_G/R = 2$ boundary which locally indicate that the boundary is acting like a temperature sink (i.e. the temperature decreases as the wall is approached). But, this is confined to the points nearest the wall and does not extend out into the flow beyond the immediate influence of the glued particles. Instead, the granular temperature is uniform in the channel centre. Thus, this effect is dominated by the microscopic lengthscales of the

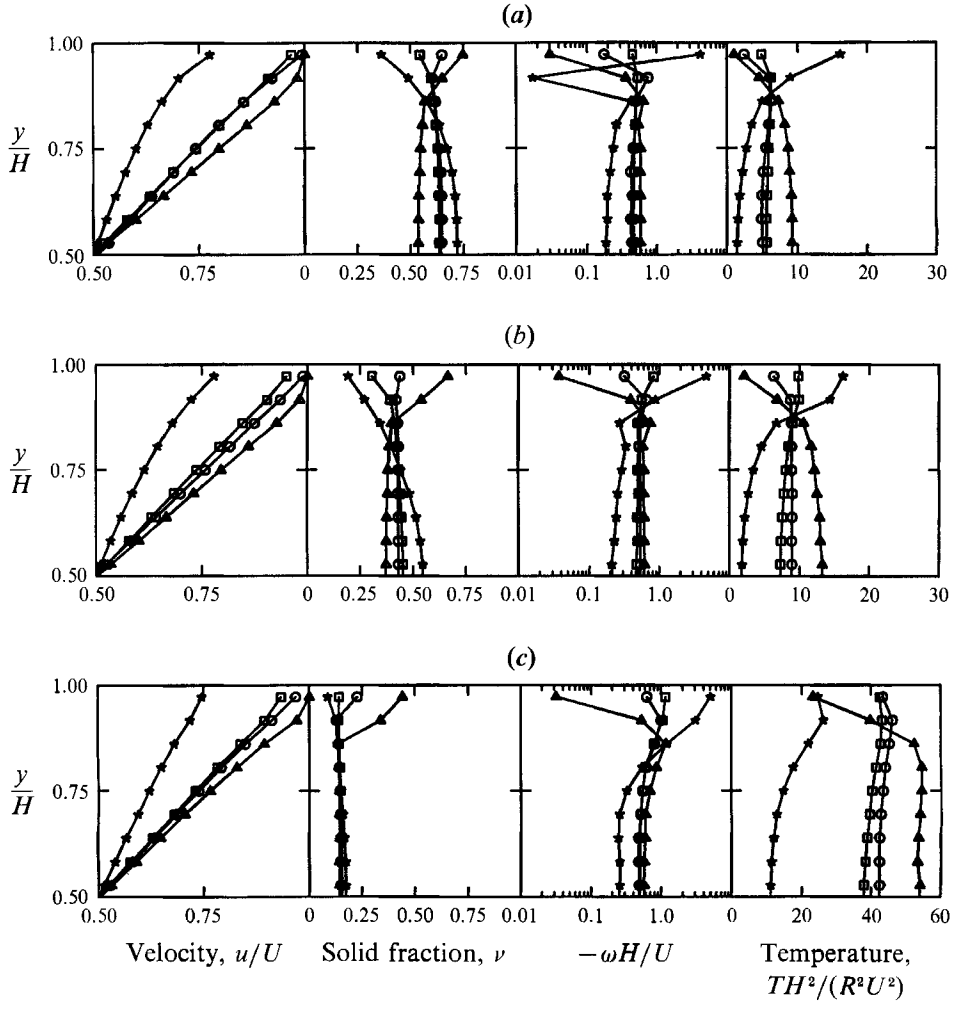

FIGURE 5. The effect of varying the glued particle size for three values of the solid concentration: (*a*) $\bar{\nu} = 0.65$, (*b*) $\bar{\nu} = 0.45$ and (*c*) $\bar{\nu} = 0.125$. For all of the roughness elements, $S_G/R_G = 8$. □, $R_G/R = 0.5$; ○, 1; △, 2; ★, smooth.

roughness size and, on continuum scales, it is inappropriate to consider the boundary as a temperature sink even though it behaves like one in the immediate vicinity of the wall. Although, this information implies that one cannot say that a wall roughened with particles that are larger than the flowing material is necessarily 'rougher' than a wall roughened with particles of the same size. (Although, it is clearly true that using smaller roughness elements leads to a smoother boundary.)

All of this discussion indicates that there is a strong interplay between the apparent characteristics of a boundary and that of the flowing material. It also raises some most basic questions regarding the application of standard continuum ideas to systems for which the boundaries cannot be considered to be infinitesimally thin, but instead extend significantly outward into the flow.

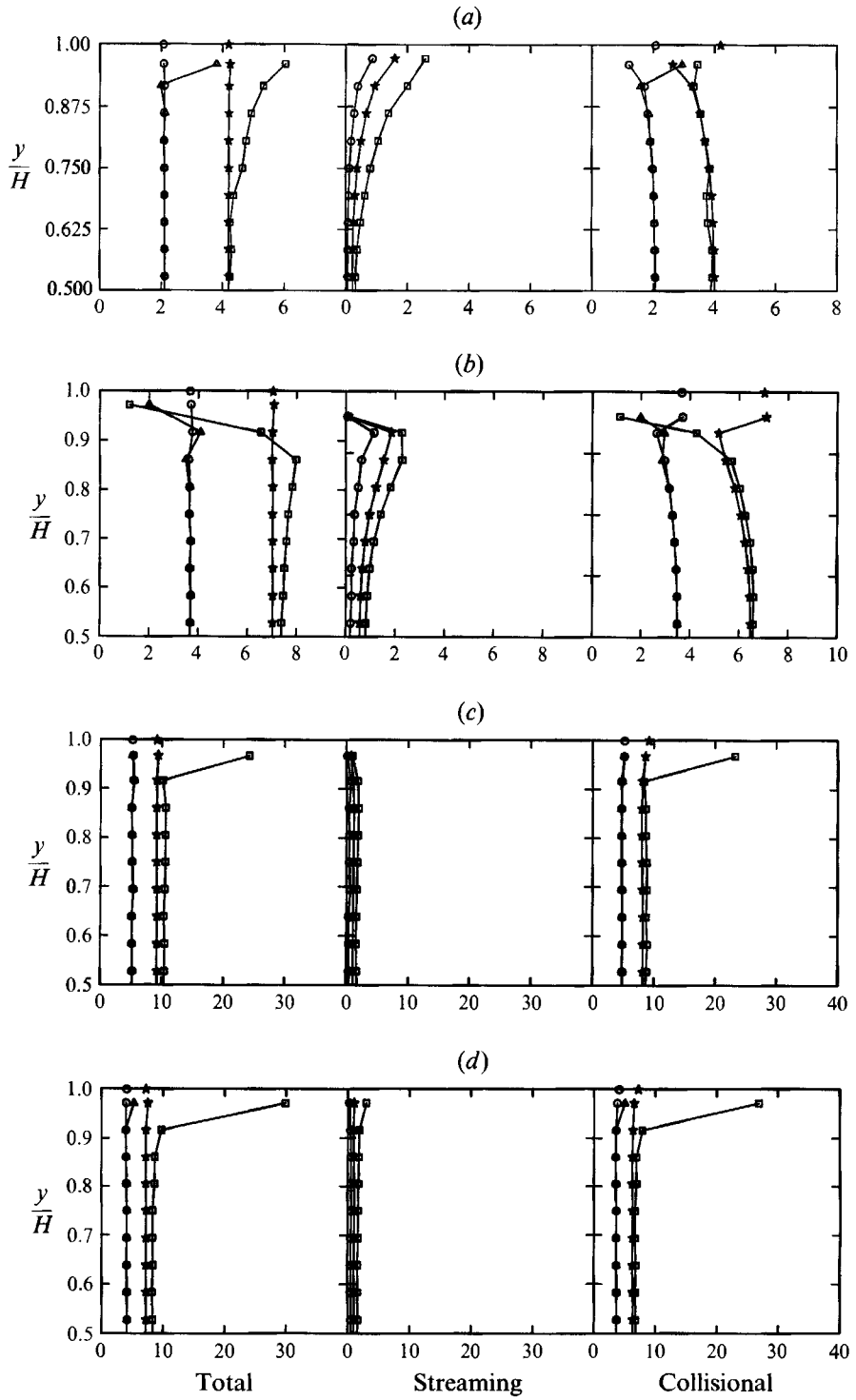

FIGURE 6. The distribution of internal stress across the channel for various glued particle spacings, $\bar{\nu} = 0.65$, $R_G/R = 1$: (*a*) smooth, (*b*) $S_G/R_G = 2$, (*c*) $S_G/R_G = 8$, (*d*) $S_G/R_G = 64$. □, τ_{xx}; ○, τ_{xy}; △, τ_{yx}; ★, τ_{yy}.

4. Internal stress distribution

Stresses are developed in a granular material by two mechanisms: (i) the Reynolds' stress-like 'streaming' contribution by which momentum is transported by particles as they follow their individual trajectories through the particle mass and (ii) the 'collisional' contribution, which reflects the momentum exchanged between particles as the result of a collision. (See Part 1 or Campbell & Gong 1986 for more details.) In Part 1, it was pointed out that one had to be very careful when averaging stress data near boundaries. The addition of roughness to the boundaries adds several new complications arising from the handling of the glued particles. Consider the streaming stresses. There, the glued particles do not possess any random motion and, hence, do not contribute to the streaming stresses. As such, it is inappropriate to consider their zero contribution in the averaging process, and, at the same time, it is inappropriate to include their contribution to the local solids concentration ν. Thus, a separate calculation of the solid fraction ν that excludes the contribution of the glued particles is used to yield the streaming stresses in the region nearest the boundary.

A similar problem arises with the calculation of the collisional stresses. There, the stresses generated by collisions with glued particles must be averaged into the local stress state of the material, even though these are boundary collisions; this is necessary since such collisions are responsible for a portion of the momentum transport in the averaging strips along each boundary. However, two data points are plotted on the top boundary ($y/H = 1$) for the τ_{xy} and τ_{yy} stresses applied by the wall. Those forces are attributed to the wall from two sources: (i) direct collisions between a particle and the wall and (ii) the forces that must be absorbed by the glue joint to hold the glued particles in place against collisions with free particles (Note that the glue joint can only withstand forces normal and tangential to the surface and thus only contribute to the τ_{xy} and τ_{yy} stresses.) Thus, the contribution of a glued–free particle collision is, itself, divided into two parts: (i) the contribution to the average that reflects the transport of momentum between the centres of the glued and free particles, which is attributed to the averaging strip nearest the wall and contributes to all four components of the stress tensor, and (ii) the forces supported by the wall across the glue joint, which is attributed to the wall and only contributes to the τ_{xy} and τ_{yy} stresses. It is in this sense that the rough boundary, as it extends into the flow field, contributes to all the components of the stress tensor, even though, on continuum scales, it may only apply shear and normal forces. (Note that this accounts for the linear motion of a glued particle attached to the wall, but cannot account for the torque applied to the particle, which must also be absorbed by the glue joint; this will be dealt with in the discussion on couple stresses that follows.)

Figures 6–8 show several examples of the stress distribution across the channel for the three mean concentrations $\bar{\nu} = 0.65$, 0.45 and 0.15, that were used in this study. As before, only the top half of the channel is shown in order that the details might be more apparent. All of these data were generated for $R_G/R = 1.0$ and various roughness spacings: (*a*) smooth, (*b*) $S_G/R_G = 2$, (*c*) $S_G/R_G = 8$ and (*d*) $S_G/R_G = 64$. For each case, the complete stress tensor is plotted along with its constituent streaming and collisional parts. Generally, these demonstrate the behaviour that one might have expected. The stresses τ_{xy} and τ_{yy} are applied at the walls and, in steady flow, must be equilibrated at the opposite boundary. Consequently, both stresses are uniform across the control volume. The other two stresses, τ_{yx} and τ_{xx}, cannot be applied by a horizontal boundary and, consequently, are self-equilibrated and

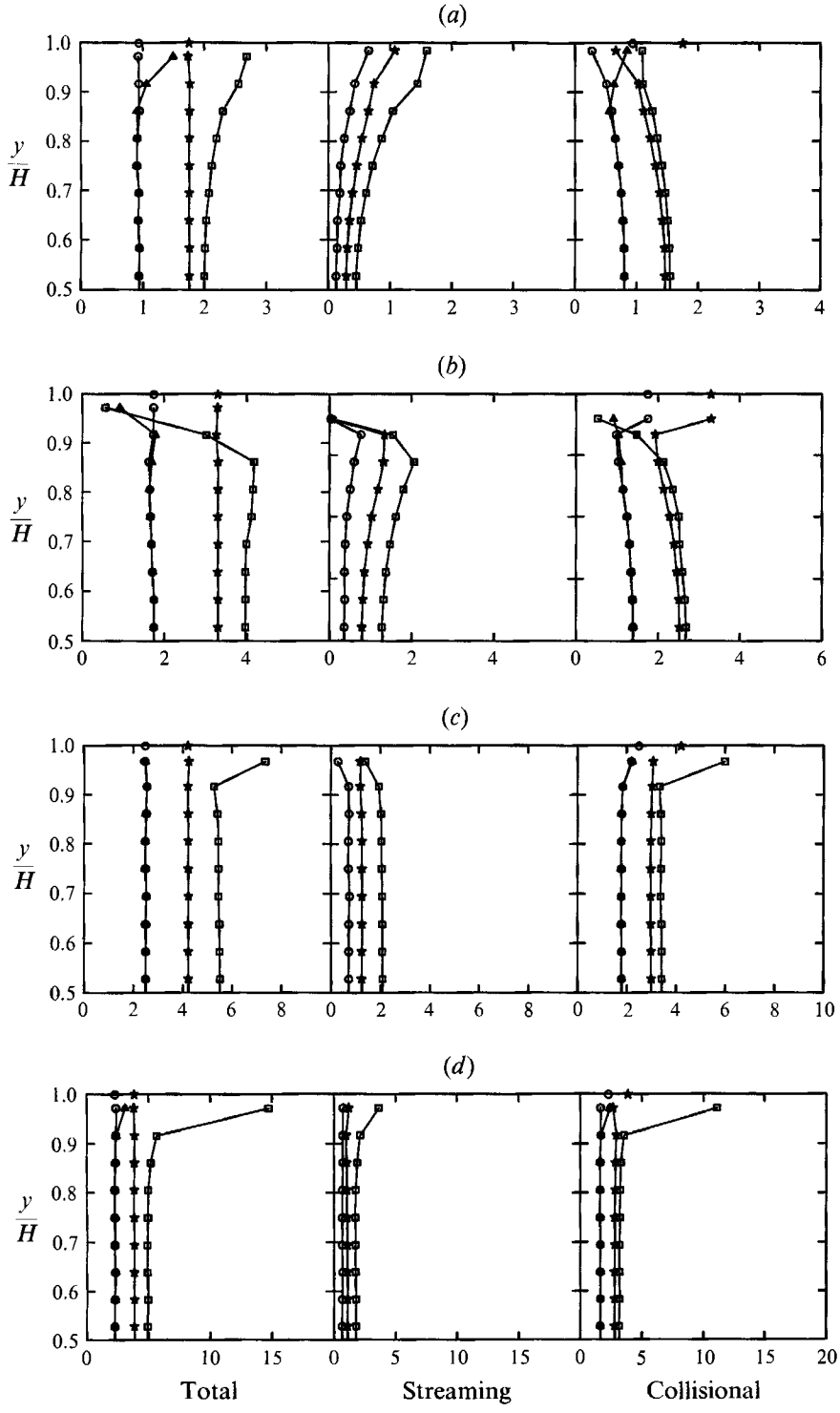

FIGURE 7. The distribution of internal stress across the channel for various glued particle spacings, $\bar{\nu} = 0.45$, $R_G/R = 1$: (*a*) smooth, (*b*) $S_G/R_G = 2$, (*c*) $S_G/R_G = 8$, (*d*) $S_G/R_G = 64$. Symbols as figure 6.

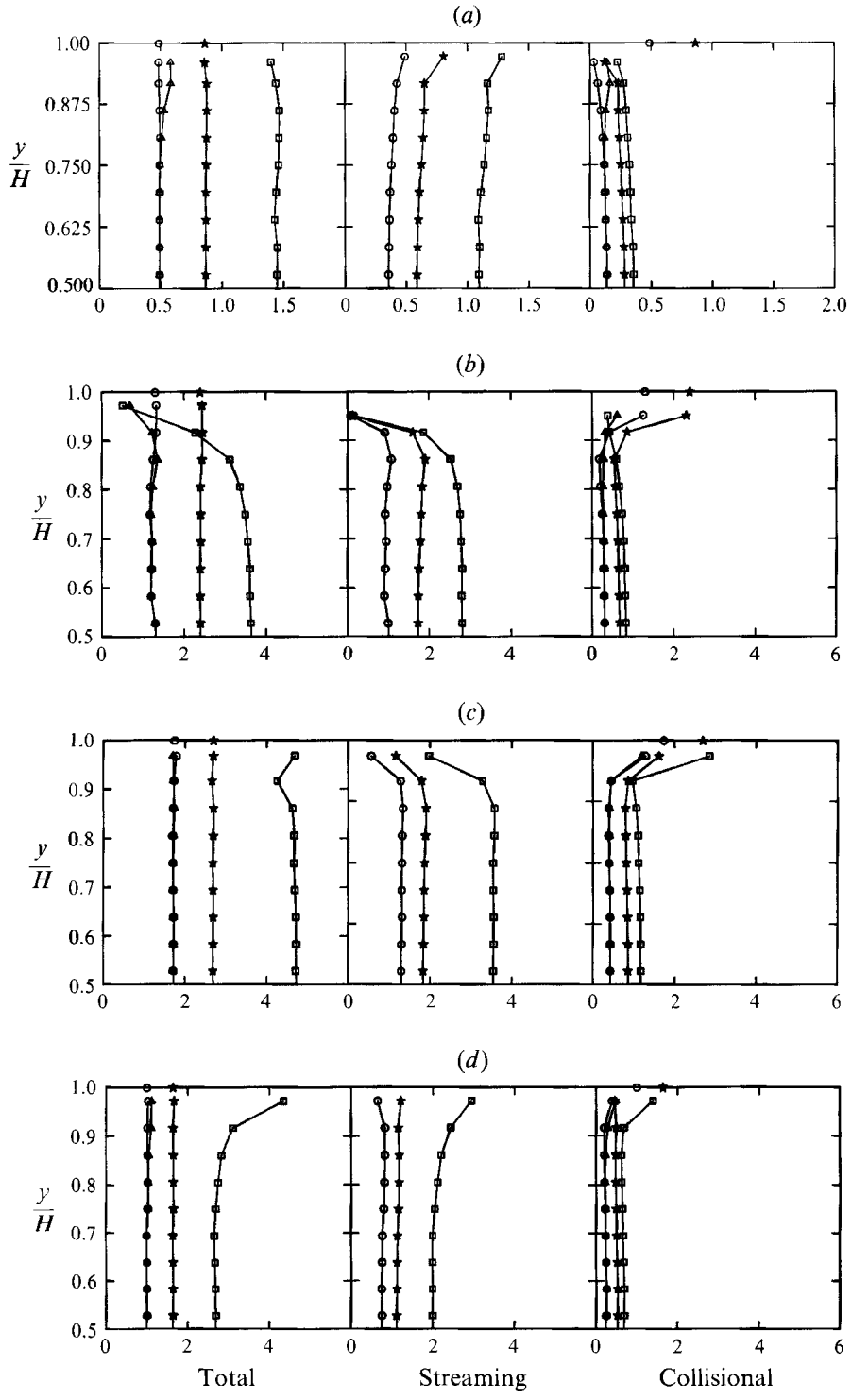

FIGURE 8. The distribution of internal stress across the channel for various glued particle spacings, $\bar{\nu} = 0.15$, $R_G/R = 1$; (*a*) smooth, (*b*) $S_G/R_G = 2$. (*c*) $S_G/R_G = 8$, (*d*) $S_G/R_G = 64$. Symbols as figure 6.

determined by the stress reaction of the material to the applied stresses. Furthermore, the larger the solid concentration, the larger the overall stress levels. Also, at $\nu = 0.15$, the largest contribution is made from the streaming stresses, while at the higher densities, the largest contribution is made by the collisional stresses. In addition, one may have been able to anticipate some of the effects of surface roughness. Naturally, the smallest stresses are observed for the smooth wall, but those are only slightly smaller than those observed for the close packed cases, $S_G/R_G = 2$; this confirms the observations, made in the last section, that the close-packed wave behaves as if it were only slightly rougher than a small wall. Increasing the 'roughness' of the wall by increasing the glued particle spacing increases the overall magnitude of the stresses.

Finally, notice that for widely spaced glued particles, i.e. $S_G/R_G \geqslant 8$, there is an anomalously large τ_{xx} stress in the strip nearest the wall. This may attributed to the lines of particles that form along the walls in front of the glued particles, such as those seen in figure 1(*d*). Such lines may be extremely long, and thus provide a very efficient mechanism of force transmission. This makes a contribution to the τ_{xx} component of the collisional stress tensor as most collisions along those lines of particles occur in the x-direction and provide an impulse that is also in the x-direction. As such, it is not surprising to see that this effect is largest for the largest mean concentrations for which one would expect that such layers might form more readily. What is somewhat surprising is that the effect is most apparent for the most widely spaced glued particles. For example, in the case of $\bar{\nu} = 0.65$, $R_G/R = 1$. $S_G/R_G = 64$, the τ_{xx} stress near the wall is nearly four times that occurring near the centre of the channel.

Perhaps the most interesting feature of these data is that the stress tensors are asymmetric near boundaries. However, roughening the boundary has a strong effect on the induced asymmetries. The largest asymmetries are observed in the smooth wall distributions (figures 6*a*–8*a*) but, as might be expected, very similar behaviour is seen for $S_G/R_G = 2$ cases (figures 6*b*–8*b*) when the roughening particles are close-packed along the walls and the flow sees a nearly smooth surface. Close examination of these figures may, hopefully only briefly, confuse the reader. In the smooth wall cases (figures 6*a*–8*a*) $\tau_{yx} > \tau_{xy}$ directly next to the wall, while exactly the opposite behaviour is seen in the $S_G/R_G = 2$ case. This is not, as it might first seem, a contradiction. A flat wall provides a τ_{xy} stress without being able to generate a balancing τ_{yx} stress, thus applying a clockwise torque to the particles. Within the layer nearest the wall, the material resists by applying a counterclockwise torque ($\tau_{yx} > \tau_{xy}$) (which corresponds to in a slope change in the rotational velocity distribution). Now consider the $S_G/R_G = 2$ cases (figures 6*b*–8*b*). There, the clockwise torques are applied by the outer edges of the roughening layer of particles which are represented, not by the points on the wall, but by the points nearest the wall. As for the smooth wall stresses, it can be seen that $\tau_{xy} > \tau_{yx}$, implying a clockwise torque; but, unlike a perfectly smooth wall, which may only exert a τ_{xy} shear stress, the gently undulating outer surface of the roughening particles can exert a small, but non-zero, τ_{yx} stress which reduces the degree of asymmetry. (Note that here the roughening particles occupy most of the first averaging strip near the wall so that geometric constraints prohibit any contribution from free–free particle collisions into these statistics; thus, only glued–free collisions, which produce large clockwise torques, are represented there.) The countertorque ($\tau_{yx} > \tau_{xy}$) is exerted by collisions between free particles in the second strip out from the wall. Consequently, in comparing the smooth wall and $S_G/R_G = 2$ figures, one should shift one's point of reference a point

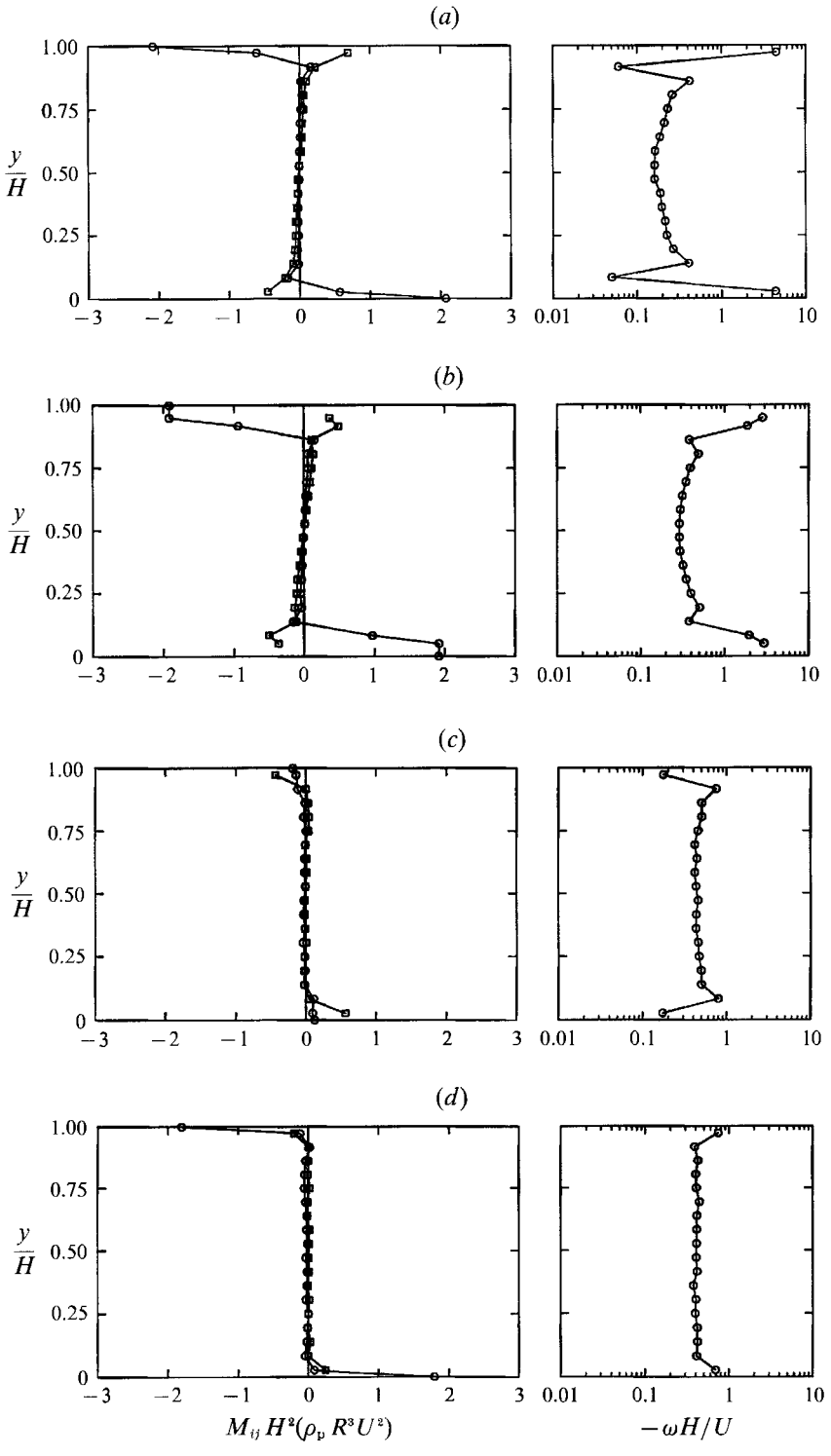

FIGURE 9. The distribution of couple stress across the channel for various glued particle spacings, $\bar{\nu} = 0.65$, $R_G/R = 1$; (*a*) smooth, (*b*) $S_G/R_G = 2$, (*c*) $S_G/R_G = 8$, (*d*) $S_G/R_G = 64$. □, M_{zx}; ○, M_{zy}.

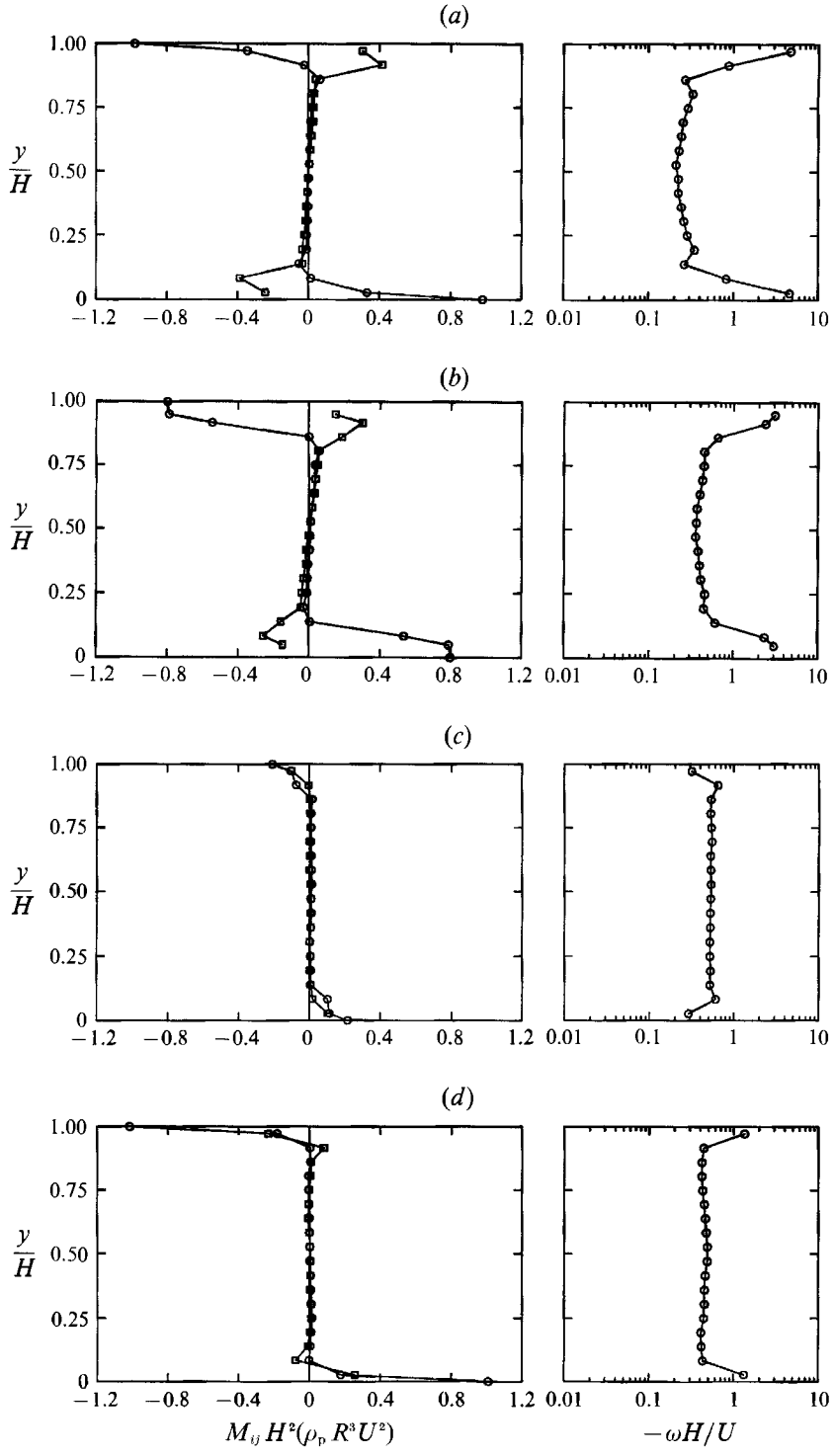

FIGURE 10. The distribution of couple stress across the channel for various glued particle spacings, $\bar{\nu} = 0.45$, $R_G/R = 1$: (*a*) smooth, (*b*) $S_G/R_G = 2$, (*c*) $S_G/R_G = 8$, (*d*) $S_G/R_G = 64$. Symbols as figure 9.

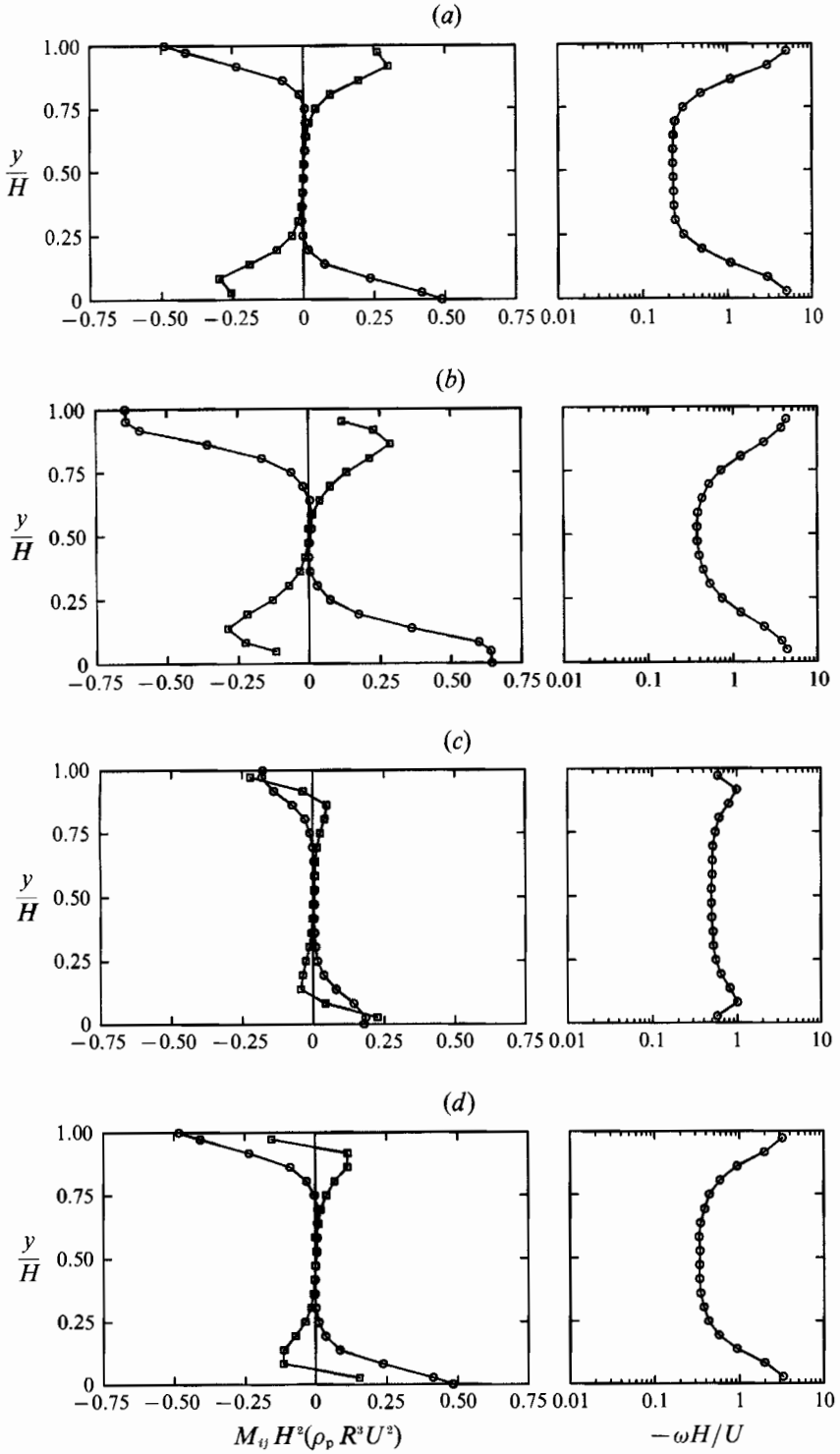

FIGURE 11. The distribution of couple stress across the channel for various glued particle spacings, $\bar{\nu} = 0.15$, $R_G/R = 1$: (*a*) smooth, (*b*) $S_G/R_G = 2$, (*c*) $S_G/R_G = 8$, (*d*) $S_G/R_G = 64$. Symbols as figure 9.

out from the walls so as to compare the wall stresses in the smooth wall cases with those in strip nearest the wall in the $S_G/R_G = 2$ cases, and the smooth wall stresses in the strip nearest the wall should be compared with the $S_G/R_G = 2$ stresses in the second strip away from the wall and so on.

However, the magnitude of the asymmetries are reduced for the rougher wall cases – in particular, the $S_G/R_G = 8$ cases (figures 6*c*–8*c*), for which the asymmetry virtually disappears. At larger spacings, e.g. $S_G/R_G = 64$ (figures 6*d*–8*d*) the wall becomes progressively smoother and the asymmetry associated with a flat wall beings to reappear. This may be accounted for by the process described in §3, in which the torques applied by the smooth portions of the boundary are balanced by countertorques applied by the glued particles. But this may also be understood by realizing that the roughness elements make these a peculiar boundary type when considered from a continuum mechanical point of view. For continuum modelling, one would want to assume that the roughening particle size is small compared to continuum scales so that the walls may be treated as flat, well-defined boundaries. As such, they may only exert shear and normal (τ_{xy} and τ_{yy}) stresses. However, the glued particles extend outward into the flow field and experience collisions with free particles that result in the generation of the other two components of the stress tensor. In this way, the rough boundary has a direct impact on all the components of the stress tensor and not just on the τ_{xy} and τ_{yy} stresses. It is not clear how to make sense of this from a continuum viewpoint, even though, on a microscopic level, the meaning is clear. Once again, this indicates that events occurring over particle scales are important near boundaries.

As was also described in Part 1, such asymmetries are only possible in steady flows in the presence of gradients in a couple stress tensor, $\boldsymbol{M}$. The couple stress distributions that correspond to the cases shown in figures 6–8 are shown in figures 9–11, respectively. Notice that only the values for the M_{zy} component (the only one that may be exerted by a flat boundary) are attributed to the walls even though a collision with a glued particle will make contributions to both couple stress components. The M_{zy} component on the boundary represents a combination of the torques that are directly exerted on free particles by wall collisions and those torques that must be absorbed by the glue joint to keep the glued particle from rotating. Also plotted are the corresponding rotational velocity distributions. As might be expected the behaviour of the rotational velocities is mirrored in the couple stresses; i.e. one sees non-zero couple stresses whenever there are gradients of rotational velocity. The general behaviour is best observed by examining the flat wall cases, where the torques applied by the wall are the largest. But, in all cases, the largest couple stresses are applied at the wall and eventually go to zero near the centre of the channel as the bulk material adjusts itself to the wall torque. Further reducing the particle concentration decreases the magnitudes of the couple stresses. Furthermore, the rapid slope changes apparent in the $\bar{\nu} = 0.65$ smooth wall data are absent from the corresponding $\nu = 0.15$ data. In concert, the large gradients of rotational velocity also disappear. Collectively, these indicate that particles are experiencing small levels of torque.

As might be expected from the stress data described earlier, the couple stress distributions react strongly to surface roughness. Since the couple stress distribution in many ways reflects the way in which the bulk material responds to the torques applied at the walls, the magnitudes will diminish along with the ability of the rough walls to apply a torque. Consequently, it should not be surprising to see that the close-packed case, $S_G/R_G = 2$, almost mirrors the smooth wall cases. Increasing the

roughness diminishes the wall torque until it has almost disappeared by $S_G/R_G = 8$. A further increase in the wall spacing results in a smoother wall and the couple stress distribution does, indeed, begin to assume the characteristics of a flat wall.

5. Conclusions

This paper has examined the effects on a granular shear flow of roughening the solid boundary surfaces by 'gluing' on particles. The first result is that the spacing of particles has a strong effect on the apparent 'roughness' of the boundary. Close-packed particles present a gently undulating surface to the flowing material and behave nearly as a flat boundary while the maximum apparent roughness is achieved when the glued particles are spaced far enough apart that the free particles have easy access to the flat wall. Further spacing of the glued particles leads to a progressively 'smoother' (i.e. more like a flat wall) boundary, although the wall retains many 'rough wall' characteristics with the glued particles spaced 64 radii apart. This is especially true at large concentrations when the glued particles draft into their service free particles that become trapped along the wall and effectively extend the range of influence of the glued roughness elements.

This indicates that one must be careful when applying roughness to the driving surfaces of shear cells or other material testing devices. To achieve a good approximation to a no-slip condition requires that the roughening particles be spaced at least a particle diameter apart. In fact, one need not worry about spacing the glued particles too far apart as separations of 32 diameters still show the characteristics of very rough walls. But the common practice of applying a layer of glue to the surface and then haphazardly pouring particles on the surface to be attached where they fall, may place particles so closely together that the surface will nearly behave as if it was smooth. Such preparations probably account for the widely disparate results derived from annular shear cells.

This paper and its companion, Campbell (1993), have two main lessons and roughening the walls has interesting implications with regards to both. The first is that the way in which a boundary applies torque to the flow particles can have a strong effect on the entire flow field. A truly 'rough' wall (such as $S_G/R_G = 8$) strongly inhibits the way in which the wall applies torque to the flowing particles. This occurs because, after experiencing a torque during collision with the wall, a free particle will receive a countertorque on a subsequent collision with a glued particle that nearly negates the torque applied by the flat section of the boundary. Another way to look at the problem is that the glued particles experience collisions with free particles in such a manner as to make contributions to all the components of the stress tensor. Thus, a rough wall influences the entire stress state of the material in its immediate vicinity; a flat wall may only influence the two components of the stress tensor in the directions normal and tangential to its surface, leaving the others arbitrary and opening the possibility of stress tensor asymmetries. As a result, much less significant stress tensor asymmetries, implying smaller internal torques, are observed in the neighbourhood of rough boundaries. At the same time the magnitude of the couple stresses is likewise reduced.

The second lesson is that, near boundaries, many events occur over microscopic lengthscales on the order of a particle diameter rather than the continuum lengthscales of the problem (such as the spacing of the driving walls). One way to explain the influence of roughness on torque transmission is that the boundary extends outward into the flow to the edges of the roughening elements. In Part 1, it

was shown that the free particle diameter became an important lengthscale in the neighbourhood of boundaries. Here, an additional lengthscale, the glued particle diameter, is also important. Also, the Type B boundary, described in Part 1, shows much the same behaviour as the rough boundaries – and for, intuitively, much the same reasons. Remember that the Type B boundary exerted its impulse at the particle centre and not at its edge, which, in a sense, implies that the Type B boundary, like the rough boundaries, extends outward into the flow, this time across the particle radius between the wall and the centre of the colliding particle.

This signals problems in attempts to derive continuum models that can accurately model such boundaries; much too much is occurring over non-continuum scales (i.e. on the order of particle sizes) and much of that has a strong effect on the nature of the flow far from the boundary. Furthermore, many of the aspects of the boundaries described in this paper are not limited to granular flows and probably occur in many multiphase flows involving solid particles.

This study was supported by the National Science Foundation under grants MEA-8352513 and CTS-8907776, with additional funding provided by the International Fine Particle Research Institute, IBM and Sun Microsystems for which the author is extremely grateful. The author would like to thank Ailing Gong for her participation in the early portions of this study and Professor J. D. Goddard for insights into couple stresses. Additional thanks are due Holly Campbell for proofreading the manuscript and to Sean, Ian and Dr Ted Geisel.

REFERENCES

CAMPBELL, C. S. 1982 Shear flows of granular materials. PhD thesis; and *Rep.* E-200.7, Division of Engineering and Applied Science, California Institute of Technology.

CAMPBELL, C. S. 1990 Rapid granular flows. In *Ann. Rev. Fluid Mech.* **22**, 57–92.

CAMPBELL, C. S. 1993 Boundary interactions for two-dimensional granular flows. Part 1. Flat boundaries, asymmetric stresses and couple stresses. *J. Fluid Mech.* **247**, 111–136.

CAMPBELL, C. S. & BRENNEN, C. E. 1985 Computer simulation of granular shear flows. *J. Fluid Mech.* **151**, 167–188.

CAMPBELL, C. S. & GONG, A. 1986 The stress tensor in a two-dimensional granular shear flow. *J. Fluid Mech.* **164**, 107–125.

CAMPBELL, C. S. & GONG, A. 1987 Boundary conditions for two-dimensional granular flows. In *Proc. Sino-US Intl Symp. on Multiphase Flows, Hangzhou, China, August, 1987*, Volume I, pp. 278–283.

CRAIG, K., BUCKHOLTZ, R. H. & DOMOTO, G. 1987 The effects of shear surface boundaries on stresses for the rapid shear of dry powders, *Trans. ASME J. Tribol.* **109**, 232–237.

HANES, D. M. & INMAN, D. L. 1985 Observations of rapidly flowing granular fluid flow. *J. Fluid Mech.* **150**, 357–380.

HANES, D.M., JENKINS, J.T. & RICHMAN, M. W. 1988 The thickness of steady plane shear flows of circular disks driven by identical boundaries. *Trans. ASME* E: *J. Appl. Mech.* **55**, 969–974.

JENKINS, J. T. & RICHMAN, M. W. 1986 Boundary conditions for plane flows of smooth, nearly elastic, circular disks. *J. Fluid Mech.* **171**, 53–69.

LOUGE, M. Y., JENKINS, J. T. & HOPKINS, M. A. 1990 Computer simulations of rapid granular shear flows between parallel bumpy boundaries. *Phys. Fluids* A **2**, 1042–1044.

RICHMAN, M. W. 1988 Boundary conditions based upon a modified Maxwellian velocity distribution for flows of identical, smooth, nearly elastic spheres. *Acta Mechanica* **75**, 227–240.

RICHMAN, M. W. & CHOU, C. S. 1988 Boundary effects on granular shear flows of smooth disks. *Z. Angew. Math. Phys.* **39**, 885–901.

RICHMAN, M. W. & MARCINIEC, R. P. 1990 Gravity-driven granular flows of smooth inelastic spheres down bumpy inclines. *Trans. ASME* E: *J. Appl. Mech.* **57**, 1036–1043.

SAVAGE, S. B. & SAYED, M. 1984 Stresses developed by dry cohesionless granular materials in an annular shear cell. *J. Fluid Mech.* **142**, 391–430.